Accelerated Molecular Dynamics of Temperature-Programed Desorption

Kelly E. Becker,[1] Maria H. Mignogna,[1] and Kristen A. Fichthorn[1,2]

[1]*Department of Chemical Engineering, The Pennsylvania State University, University Park, Pennsylvania 16802, USA*
[2]*Department of Physics, The Pennsylvania State University, University Park, Pennsylvania 16802, USA*

(Received 4 October 2008; published 29 January 2009)

We use accelerated molecular dynamics to simulate temperature-programed desorption (TPD) of *n*-pentane from the basal plane of graphite in the first atomistic simulations to probe TPD over laboratory time scales. Although the simulated TPD spectra agree with experiment, a detailed analysis reveals underlying kinetic phenomena that contrast the standard experimental interpretation and opens new possibilities for understanding molecular kinetics at solid surfaces.

DOI: 10.1103/PhysRevLett.102.046101 PACS numbers: 68.43.Nr, 68.43.Vx, 82.20.Db

The thermal desorption of adsorbed species from solid surfaces occurs in nearly every application involving adsorption, including catalysis, assembly at surfaces, wetting, etching, thin-film growth, and lubrication. The most widely used experimental method for quantifying thermal desorption is temperature-programed desorption (TPD). In TPD, molecules are adsorbed onto a solid surface with an initial temperature T_0 and coverage θ_0. The surface is heated with a rate β, such that the surface temperature T changes with time t according to $T = T_0 + \beta t$. The intensity of desorbing molecules $d\theta/dt$ yields a TPD spectrum that reflects the desorption rate. For first-order desorption, we have

$$\frac{d\theta}{dt} = -k(\theta, T)\theta, \tag{1}$$

where k is the rate constant, with the approximate Polanyi-Wigner form $k = \nu_0 e^{-E_d/kT}$. Here ν_0 is the prefactor and E_d is the activation energy. Although several methods have been proposed to extract kinetic parameters from experimental TPD spectra [1–6], interpretation of TPD can still be controversial. A good example of this controversy can be found in TPD studies of *n*-alkane desorption [7–13], which is the subject of this Letter.

A significant difficulty with interpreting TPD is that this macroscopic experiment offers a limited picture of the underlying microscopic kinetic events. In this regard, theory and simulation could be useful—although, heretofore, modeling efforts have been limited to lattice-based approaches [14–18]. Because adsorption may not be localized to binding sites at temperatures where thermal desorption is significant, the validity of lattice models is questionable. This difficulty is compounded for large molecules, whose various conformational states do not easily map to a lattice.

In this Letter, we present real-space, atomic-scale simulations based on accelerated molecular dynamics (MD) [19–21] that can probe TPD over laboratory time scales. We focus on the desorption of *n*-pentane (C_5H_{12}) from the basal plane of graphite C(0001). To model the adsorption of pentane on C(0001), we use an all-atom representation for pentane. Intermolecular and intramolecular potentials are taken from the OPLS force field [22] and are described in detail elsewhere [13]. The highest frequency modes, i.e., bond stretches and H − C − H angle bends, are constrained using the RATTLE algorithm [23]. All other internal motions, including C − C − C and H − C − C bends and all torsions, are included explicitly. Interactions between the pentane molecules and the graphite surface are dominated by dispersion forces and modeled using a modified Steele's potential [13,24].

To simulate the accelerated MD of TPD, we employ a variant of the Bond-Boost method [21]. We take advantage of the fact that desorption is significantly slower than other surface processes (e.g., surface diffusion, *trans-gauche*, and interlayer transitions) so that these fast processes are in equilibrium on the time scale of desorption. A boost potential ΔV is applied to all N adsorbed molecules, such that the adlayer is simulated with a modified potential given by $V^* = V + \Delta V$, where $V[= V(\mathbf{R})]$ is the original potential, which is a function of the system configuration $\{\mathbf{R}\}$. The boost potential has the form

$$\Delta V(\mathbf{R}) = \frac{A(\mathbf{R})}{N} \sum_{i=1}^{N} \delta V_i(\mathbf{R}). \tag{2}$$

Here, $\delta V_i(\mathbf{R}) = (\alpha_1 - 1)V_{s,i}(\mathbf{R}) + (\alpha_2 - 1)V_{\text{inter},i}(\mathbf{R})$, where $V_{s,i}$ and $V_{\text{inter},i}$ are the molecule-surface and molecule-molecule interaction for molecule i, respectively. We used $\alpha_1 = 0.1$ and $\alpha_2 = 0.35$, values that were selected to accelerate desorption (by weakening V_s and V_{inter} on V^*), while probing the same phase space as canonical simulations on the original potential V. The phase-space overlap was confirmed by the overlap of energy histograms obtained on V and on V^*, as well as by matching radial distribution functions at all conditions probed. The envelope function $A(\mathbf{R})$ $[\equiv A(\epsilon_{\max})]$ is given by

$$A(\epsilon_{\max}) = \begin{cases} 1 - (\frac{\epsilon_{\max}}{q})^2, & \epsilon_{\max} \le q \\ 0, & \epsilon_{\max} > q. \end{cases} \tag{3}$$

Here, $\epsilon_{\max} = MAX\{|(z_{\mathrm{com},i} - z_e)/z_e|\}$, where $z_{\mathrm{com},i}$ is the center-of-mass height of molecule i and $z_e (= 3.44$ Å) is the equilibrium height of a first-layer molecule. $q (= 2.57)$ is a dimensionless threshold defined such that V_s is negligible for any possible orientation of a desorbing molecule near q. In addition to ensuring that $\Delta V \rightarrow 0$ at the transition state [20,21], A channels the boost into the molecule closest to desorbing.

Our simulations proceed as follows: We equilibrate an n-pentane layer on the surface at some fraction of a full monolayer (ML) θ_0. The ML coverage ($\theta = 1$) is based on the unit cell for pentane resolved in neutron diffraction experiments by Kruchten *et al.* [25], which we can reproduce. Subsequent to equilibration, we apply the boost until $\epsilon_{\max} > q$. At this point, desorption occurs, the remaining molecules are briefly simulated with regular MD, the boost is reapplied, and the cycle continues.

The physical time t_{i+1} for the $(i+1)^{\mathrm{st}}$ MD time step is given by $t_{i+1} = t_i + \Delta t e^{\Delta V_i/kT}$, where Δt is the MD time step and ΔV_i is given by Eq. (2). The temperature is increased by $T = T_0 + \beta t$ using the Berendsen thermostat [26]. During the simulation, we record $\theta(t)$ and fit the average from 10 runs to a polynomial. We obtain the TPD spectrum analytically from $-d\theta/dt$.

To verify our model, we simulated TPD beginning with $\theta_0 = 1$ using $\beta = 2.0$ K/s. Paserba and Gellman probed pentane desorption from C(0001) experimentally under these conditions [9] and a comparison between our simulated spectrum and theirs is shown in Fig. 1. As we see in Fig. 1, the leading edges of the spectra are close and the peak temperatures agree within $\sim 1^{\circ}$. Differences in the initial portions of the spectra can be attributed to differences in coverage calibration between simulation and experiment. Further, it is likely that the rapid drop-off of the simulated TPD spectrum compared to experiment is due to the absence of surface defects in the simulations. Tait *et al.* found that surface defects, which bind alkanes more strongly than sites on the perfect C(0001) surface, influence TPD spectra for coverages below ~0.2–0.3 ML [12]. By binding molecules more strongly, defects delay low-coverage desorption to higher temperatures and broaden the experimental TPD spectrum.

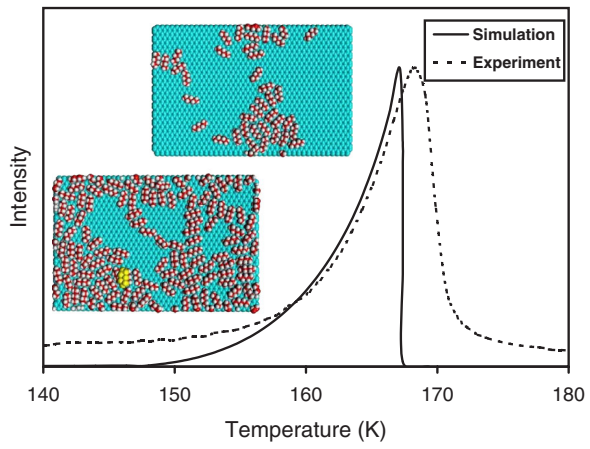

FIG. 1 (color online). Comparison of a simulated TPD spectrum with $\beta = 2.0$ K/s for $\theta_0 = 1.0$ ML to an experimental spectrum [9]. Both spectra are scaled so the maximum intensity is one. The insets show snapshots for $\theta = 0.75$, with a second-layer molecule (yellow or light), and $\theta = 0.25$.

Figure 2 shows simulated TPD spectra with $\beta = 0.6$ K/s. For $\theta_0 = 1.0$, the simulated time is almost 40 s. The spectra for $\theta_0 = 0.5$–1.0 take on the appearance of those obtained experimentally by Tait *et al.* [12] for n-butane (C_4H_{10}) and n-hexane (C_6H_{14}) on C(0001) using $\beta = 0.6$ K/s. Although it is reasonable to attribute the increasing peaks of the simulated spectra with θ_0 to attraction between the pentane molecules, as was done in Tait's study [12], we will show below that this analysis does not completely capture the underlying physics. We surmise that the "breakthrough" of the simulated TPD spectrum for $\theta_0 = 0.25$, which is not seen in Tait's experimental study, is due to our neglect of surface defects, as discussed above. Finally, we note that the TPD spectra in Figs. 1 and 2 take on a zero-order appearance, which has also been noted in experimental studies of short alkanes and other physically adsorbed species [12,27]. We will return to this point below.

To obtain rate constants from our simulated TPD spectra, we employ a variant of Eq. (1), given by

$$k(\theta, T) = -\frac{1}{\theta}\frac{d\theta}{dt}. \tag{4}$$

This analysis can be done experimentally [3–6] if $\theta(t)$ is precisely known. The inset of Fig. 2 shows a plot of Eq. (4) obtained from the TPD spectra in Fig. 2. If k was independent of coverage, then the curves would be straight lines

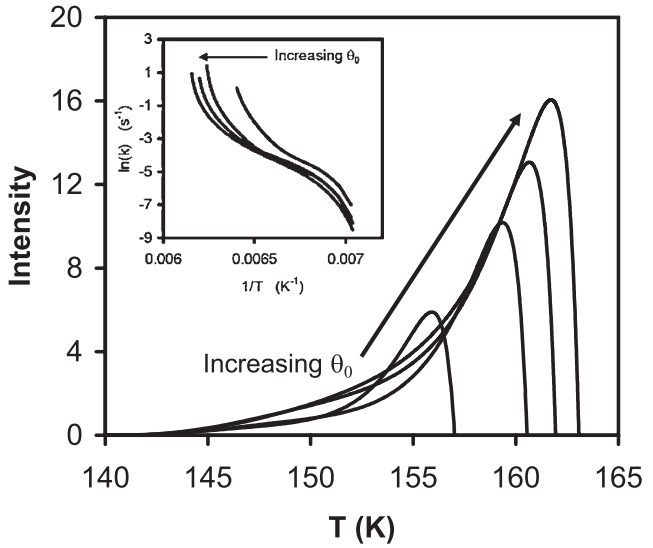

FIG. 2. Simulated TPD spectra with $\beta = 0.6$ K/s for $\theta_0 = 0.25$, 0.5, 0.75, and 1.0 ML. The inset shows the rate constants obtained from the TPD spectra using Eq. (4).

TABLE I. Prefactors ν_0 (s^{-1}) and energy barriers E_d (kJ/mol) for various coverages θ obtained from the simulated TPD spectra using Eq. (4). The uncertainties are the standard deviation in a least-squares fit of the Arrhenius plot.

θ	$\log_{10}(\nu_0)$	E_d
0.10	14.8 ± 0.8	46.0 ± 2.0
0.25	16.3 ± 0.4	52.0 ± 1.0
0.30	16.7 ± 0.3	53.0 ± 1.0
0.40	17.6 ± 0.3	56.0 ± 1.0
0.50	17.4 ± 0.2	55.8 ± 0.7
0.60	17.2 ± 0.3	55.3 ± 0.8
0.75	16.9 ± 0.8	54.0 ± 2.0
0.80	16.6 ± 0.8	54.0 ± 2.0
0.90	15.5 ± 0.3	50.4 ± 0.9

that would superimpose exactly. However, this is not the case. By simulating TPD spectra with various θ_0 and β ranging from 0.5–5.0 K/s, we find $k(\theta, T)$ using Eq. (4). From Arrhenius plots of $k(T)$ at fixed θ, we obtained the desorption energies and prefactors in Table I.

Table I shows that both E_d and ν_0 vary substantially with coverage and both exhibit a maximum at $\theta = 0.4$. In their experimental study of pentane on graphite, Paserba and Gellman assumed $\nu_0 = 10^{19.6}$ s^{-1} and found $E_d =$ 65.5 kJ/mol [9]. Tait and colleagues reanalyzed Paserba and Gellman's TPD data for pentane assuming upper and lower bounds for the prefactor [12] and our values in Table I fall within their estimated range [12]. However, Tait *et al.* assumed a constant prefactor and found that E_d increases with coverage for butane and hexane [12].

To understand the trends in Table I, we simulated desorption from layers at fixed coverages of $\theta = 0.25$, 0.5, 0.75, and 1.0. For each temperature and coverage, between 170 and 330 desorptions were simulated to obtain the distribution of desorption times. Generally, we expect the time distribution to be exponential for rare events, such as thermal desorption. Here, the time distributions are multiexponential, with a form given by $P(t) = \sum_j a_j e^{-k_j t}$. For example, Fig. 3 shows a time distribution at 1 ML, which indicates two distinct rate processes. From the slopes of the best-fit lines for short and long times, we found rate constants for these processes. Figure 4 shows these, along with other rate constants that we found.

Overall, we could resolve three different rate processes. The fastest of these is seen the most clearly for 1 ML and is associated with the desorption of molecules from on top of the layer. The insets in Fig. 3 show such a second-layer molecule. From the Arrhenius plot in Fig. 4, we find $E_d =$ 32.5 kJ/mol and $\nu_0 = 9.2 \times 10^{11}$ s^{-1} for second-layer desorption. If we use these values to simulate TPD with a heating rate of $\beta = 2.0$ K/s, as Paserba and Gellman used in their experimental TPD studies of pentane multilayers on C(0001), we obtain a peak temperature of 137 K—close to their value of 133 K [9]. Interestingly, we also observed

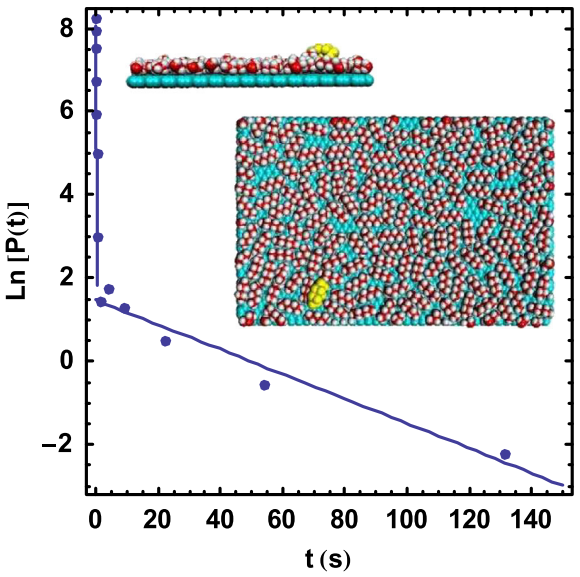

FIG. 3 (color online). Distribution of desorption times at 160 K for $\theta = 1.0$ ML. The insets show top-down and side views of a ML on C(0001) with a second-layer molecule (yellow or light color) prior to its desorption.

second-layer desorptions at lower θ. The inset to Fig. 1 shows a second-layer molecule poised to desorb at 0.75 ML. In experimental analysis of TPD spectra, such events are associated with low-temperature, multilayer desorption. Here, we find that weakly bound, second-layer molecules exist and desorb at submonolayer coverages.

The second-fastest process is desorption of isolated molecules, which is most easily observed at $\theta = 0.25$. The inset to Fig. 1 shows a snapshot with isolated molecules at 0.25 ML. From the Arrhenius plot in Fig. 4, we find

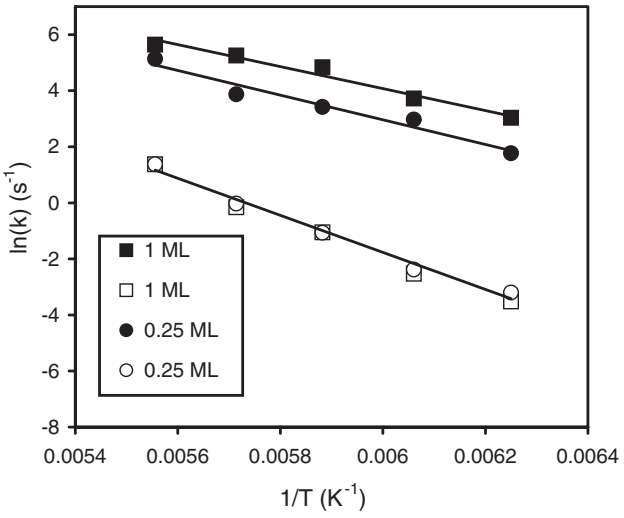

FIG. 4. Arrhenius plot of the fast (filled symbols) and slow (open symbols) processes obtained from the time distributions for fixed-coverage simulations with $\theta = 0.25$ and 1.0 ML. The uncertainties are smaller than the symbol sizes.

$E_d = 36.5$ kJ/mol and $\nu_0 = 5.5 \times 10^{12}$ s^{-1} for isolated molecules. These values are substantially smaller than experimental values (as well as the values in Table I), indicating that attractive alkane interactions play a significant role in determining the value of the desorption energy—even at low θ. The slowest time scales, which are similar for all the coverages studied, can be attributed to desorption from adsorbate islands. From the Arrhenius plot in Fig. 4, we find $E_d = 58.1$ kJ/mol and $\nu_0 = 2.4 \times 10^{17}$ s^{-1} for molecules within islands.

The large prefactor for island desorption reflects the loss of rotational entropy for molecules packed into islands relative to the free-molecule transition state. Our prefactor for island desorption falls within the range predicted by Tait *et al.* [12], who used analytical approximations to bracket possible values for ν_0 between $10^{15.3}$–10^{20} s^{-1}. Our prefactors for isolated and second-layer molecules fall below Tait's range—perhaps because their assumptions for the partition functions do not apply to these weakly bound molecules. Additionally, our rate constants are most likely effective values that represent more than one process. Although most of the time distributions indicate some degree of curvature at both short and long times (cf. Fig. 3), hinting at the presence of more than one fast or slow process, we could not resolve these processes separately.

Thus, our simulations indicate that thermal desorption can be a complex process consisting of different types of events. The net rate at a given coverage is a combination of the rates for these events. At low coverages, most of the desorptions are from isolated molecules and the fraction of these decreases with increasing θ. The increase in the activation energy with θ at low-coverage reflects the increasing population of island molecules and the increase in the prefactor indicates the loss of entropy when molecules are incorporated into islands. As the coverage increases above 0.5 ML, second-layer desorption occurs with increasing frequency and coexists with (declining) isolated desorptions, as well as slow, island desorption. Because of the weak binding of second-layer molecules and the significant entropy gain when a molecule climbs from the first to the second layer, the apparent activation energy and prefactor decline at high coverages. The fact that we are able to observe and quantify desorption from all possible types of surface environments can be taken as evidence that desorption is first order here. The coverage-dependence of k, which increases with decreasing θ, leads to TPD spectra with a zero-order appearance.

In closing, we emphasize that while our simulated TPD spectra agree with those in experiment [9,12], our interpretation of them is considerably different than the seemingly straightforward experimental interpretation. Detailed simulations and analysis along the lines utilized here could be useful in a variety of applications that rely on TPD data to resolve the impact of atomic-scale processes on macroscopic rate phenomena.

We thank Andy Gellman for providing the experimental data in Fig. 1 and Bruce Kay and Greg Kimmel for critical comments. This work was funded by the National Science Foundation, grants DGE 9987589 and DMR 0514336.

[1] P. A. Redhead, Vacuum **12**, 203 (1962).
[2] C. M. Chan, R. Aris, and W. H. Weinberg, Appl. Surf. Sci. **1**, 360 (1978).
[3] E. Habenschaden and J. Kuppers, Surf. Sci. **138**, L147 (1984).
[4] D. A. King, T. E. Madey, and J. T. Yates, Jr., J. Chem. Phys. **55**, 3236 (1971).
[5] J. L. Taylor and W. H. Weinberg, Surf. Sci. **78**, 259 (1978).
[6] J. B. Miller *et al.*, J. Chem. Phys. **87**, 6725 (1987).
[7] S. Wetterer *et al.*, J. Phys. Chem. B **102**, 9266 (1998).
[8] A. Bishop, G. Girolami, and R. Nuzzo, J. Phys. Chem. B **104**, 754 (2000).
[9] K. Paserba and A. Gellman, Phys. Rev. Lett. **86**, 4338 (2001); J. Chem. Phys. **115**, 6737 (2001).
[10] K. A. Fichthorn and R. A. Miron, Phys. Rev. Lett. **89**, 196103 (2002).
[11] R. Z. Lei, A. J. Gellman, and B. E. Koel, Surf. Sci. **554**, 125 (2004).
[12] S. L. Tait, Z. Dohnálek, C. T. Campbell, and B. D. Kay, J. Chem. Phys. **125**, 234308 (2006).
[13] K. E. Becker and K. A. Fichthorn, J. Chem. Phys. **125**, 184706 (2006).
[14] J. L. Sales, G. Zgrablich, and V. P. Zhdanov, Surf. Sci. **209**, 208 (1989).
[15] E. S. Hood, B. H. Toby, and W. H. Weinberg, Phys. Rev. Lett. **55**, 2437 (1985).
[16] S. J. Lombardo and A. T. Bell, Surf. Sci. Rep. **13**, 3 (1991).
[17] B. Meng and W. H. Weinberg, J. Chem. Phys. **100**, 5280 (1994).
[18] B. Lehner, M. Hohage, and P. Zeppenfeld, Chem. Phys. Lett. **379**, 568 (2003).
[19] E. Grimmelmann, J. Tully, and E. Helfand, J. Chem. Phys. **74**, 5300 (1981).
[20] A. F. Voter, Phys. Rev. Lett. **78**, 3908 (1997); J. Chem. Phys. **106**, 4665 (1997).
[21] R. A. Miron and K. A. Fichthorn, J. Chem. Phys. **119**, 6210 (2003); Phys. Rev. Lett. **93**, 128301 (2004).
[22] W. L. Jorgensen, D. S. Maxwell, and J. Tirado-Rives, J. Am. Chem. Soc. **118**, 11 225 (1996).
[23] H. C. Andersen, J. Comput. Phys. **52**, 24 (1983).
[24] W. A. Steele, Surf. Sci. **36**, 317 (1973).
[25] F. Kruchten *et al.*, Langmuir **21**, 7507 (2005).
[26] H. J. C. Berendsen *et al.*, J. Chem. Phys. **81**, 3684 (1984).
[27] H. J. Kreuzer and S. H. Payne, Surf. Sci. **200**, L433 (1988).